

## Supporting Information

### **The Role of Connectivity on Significant Bandgap Narrowing for Fused-Pyrene based Non-Fullerene Acceptors toward High-Efficiency Organic Solar Cells**

*Shungang Liu, Wenyan Su, Xianshao Zou, Xiaoyan Du, Jiamin Cao,\* Nong Wang, Xingxing Shen, Xinjian Geng, Zilong Tang, Arkady Yartsev, Maojie Zhang,\* Wolfgang Gruber, Tobias Unruh, Ning Li, Donghong Yu\*, Christoph J. Brabec, and Ergang Wang\**

#### **1. General characterization**

#### **2. Device fabrication and measurements**

#### **3. TGA**

#### **4. Temperature-dependent UV-vis spectra**

#### **5. CV**

#### **6. Density functional theory calculations**

#### **7. Optimization of device performance**

#### **8. Absorption spectra of PTB7-Th:PFIC6 blend films**

#### **9. XRD**

#### **10. DSC**

#### **11. PL spectra**

#### **12. Space charge limited current (SCLC) measurements**

#### **13. AFM height images**

## 1. General characterization

$^1\text{H}$  and  $^{13}\text{C}$  NMR spectra were measured on a Bruker Avance-500 spectrometer or Varian Inova 400 MHz NMR spectrometer. Mass spectra were measured on a Bruker Biflex III MALDI TOF. IR was measured on a FT-IR Spectrometer (Perkin Elmer). UV-vis absorption spectra were recorded on a UV-Vis-NIR Spectrophotometer of Agilent Technologies Cary Series. Thermogravimetric analysis was measured on a Mettler Toledo TGA/DSC 3+ Thermal Analyzer under a nitrogen flow at a heating rate of  $10\text{ }^\circ\text{C}/\text{min}$ . Differential scanning calorimetry (DSC) was recorded on a Mettler Toledo DSC 2 differential scanning calorimeter under a nitrogen flow at a heating rate of  $10\text{ }^\circ\text{C}/\text{min}$ . Cyclic voltammetry (CV) measurements were conducted on a CH-Instruments 650A Electrochemical Workstation under nitrogen in an anhydrous acetonitrile solution of tetra-*n*-butylammonium hexafluorophosphate (0.1 M). A glassy carbon electrode was used as the working electrode, a platinum-wire was used as the counter electrode, and a  $\text{Ag}/\text{Ag}^+$  electrode was used as the reference electrode. All potentials were corrected against  $\text{Fc}/\text{Fc}^+$  redox couple. The geometries of the ground states of FPIC6 and FPIC5 were optimized by density functional theory (DFT), and then the excited-state energies were calculated by time-dependent DFT (TDDFT). All the calculations were carried out using the B3LYP functional and 6-31G(d, p) basis set with the Gaussian-09 package. Photoluminescence (PL) spectra were taken on an Edinburgh Instrument FLS 980. The GIWAXS patterns were collected with the highly customized Versatile Advanced X-ray Scattering instrument Erlangen (VAXSTER) at the institute for Crystallography and Structural Physics, FAU, Germany. The system is equipped with a MetalJet D2 70 kV X-ray source from EXCILLUM, Sweden. The beam was shaped by a 150 mm Montel optics (INCOATEC, Geesthacht) and two of the available four double-slit systems with the last slit system equipped with low scattering blades (JJXray/SAXSLAB). Aperture sizes were ( $0.7 \times 0.7\text{ mm}^2$ ,  $0.4 \times 0.4\text{ mm}^2$ ) for GIWAXS. The sample position was located within the fully evacuated detector tube. The hybrid-pixel 2D Pilatus 300K detector (Dectris Ltd., Baden, Switzerland) was used to collect the scattered radiation. The measurements were carried out at energy of 9.24 keV. TR-PL Characterization was conducted by using a Ti:sapphire laser (Spectra-Physics, Tsunami) at 800 nm as an excitation source with repetition rate of 80 MHz and pulse duration of 100 fs. Frequency-doubled light (400 nm, generated by Photop

Technologies, Tripler TP-2000B) was used for excitation. Two 1 in. quartz plano-convex lenses of 50 mm focal length were used to collect PL and focused on the input slit of a spectrograph (Chromex). A streak camera (Hamamatsu C6860) with a slit width of 20  $\mu\text{m}$  was used to collect the output of the spectrograph. Background correction of the measured PL images was performed first and then the shading and spectral sensitivity correction was carried out with calibrated reference light source (Ocean Optics, LS-1-CAL). All measurements were carried out at room temperature. Atomic force microscopy (AFM) measurements were performed on a Dimension 3100 (Veeco). Transmission electron microscopy (TEM) was performed using a Tecnai G2 F20 S-TWIN instrument at 200 kV accelerating voltage.

## 2. Device fabrication and measurements

Organic solar cells with an inverted device structure of ITO/ZnO/PFN-Br/PTB7-Th:FPIC6/MoO<sub>3</sub>/Al were fabricated under conditions as follows: patterned indium tin oxide (ITO)-coated glass with a sheet resistance of 10-15  $\Omega \text{ sq}^{-1}$  was cleaned by a surfactant scrub and then underwent a wet-cleaning process inside an ultrasonic bath, beginning with deionized water followed by acetone and isopropanol. After oxygen plasma cleaning for 10 min, the ZnO layer with a thickness of 30 nm was deposited by spin-coating under 2000 rpm for 60 s on top of the ITO substrate. ZnO nanoparticles were synthesized followed the literature.<sup>[1]</sup> The poly[(9,9-bis(3'-(N,N-dimethyl)-N-ethylammonium-propyl)-2,7-fluorene)-alt-2,7-(9,9-dioctylfluorene)]dibromide (PFN-Br) was then deposited on top of the ZnO layer by spin-coating a methanol solution with a concentration of 0.5 mg/mL under 3000 rpm for 60 s. The active layer was then deposited on top of the PFN-Br layer by spin-coating a blend chloroform solution of PTB7-Th:FPIC6 (dissolved 4 h under 45 °C). Finally, 10 nm MoO<sub>3</sub> and 80 nm Al were successively deposited on the photosensitive layer under vacuum at a pressure of ca.  $4 \times 10^{-4}$  Pa, and through a shadow mask to determine the active area of the devices (0.04 cm<sup>2</sup>).

The photovoltaic performance of the OSCs were measured under a illumination of AM 1.5G (100 mW/cm<sup>2</sup>) using a SSF5-3A solar simulator (AAA grade, 50  $\times$  50 mm<sup>2</sup> photobeam size) of Enli Technology CO., Ltd.. A 2 $\times$ 2 cm<sup>2</sup> monocrystalline silicon reference cell (SRC-

00019) was purchased from Enli Technology CO., Ltd. The EQE was measured by Solar Cell Spectral Response Measurement System QE-R3011 of Enli Technology CO., Ltd. The light intensity at each wavelength was calibrated with a standard single crystal Si photovoltaic cell.

The structure of hole-only devices is ITO/PEDOT:PSS/active layer/MoO<sub>3</sub>/Al. A 30 nm thick PEDOT:PSS layer was formed on ITO substrates by spin coating an aqueous dispersion onto ITO glass (4000 rpm for 30 s). PEDOT:PSS coated substrates were dried at 150 °C for 10 min. A blend chloroform solution of PTB7-Th:FPIC6 was spin-coated onto PEDOT:PSS layer. Finally, MoO<sub>3</sub> (~6 nm) and Al (~100 nm) were successively evaporated onto the active layer under a shadow mask (pressure ca.  $4 \times 10^{-4}$  Pa). *J-V* curves were measured with a computerized Keithley 2420 SourceMeter in the dark.

The structure of electron-only devices is ZnO/active layer/Ca/Al. A blend chloroform solution of PTB7-Th:FPIC6 was spin-coated onto ZnO. Ca (~5 nm) and Al (~100 nm) were thermally evaporated under a shadow mask (pressure ca.  $10^{-4}$  Pa). *J-V* curves were measured with a computerized Keithley 2420 SourceMeter in the dark.

### 3. TGA

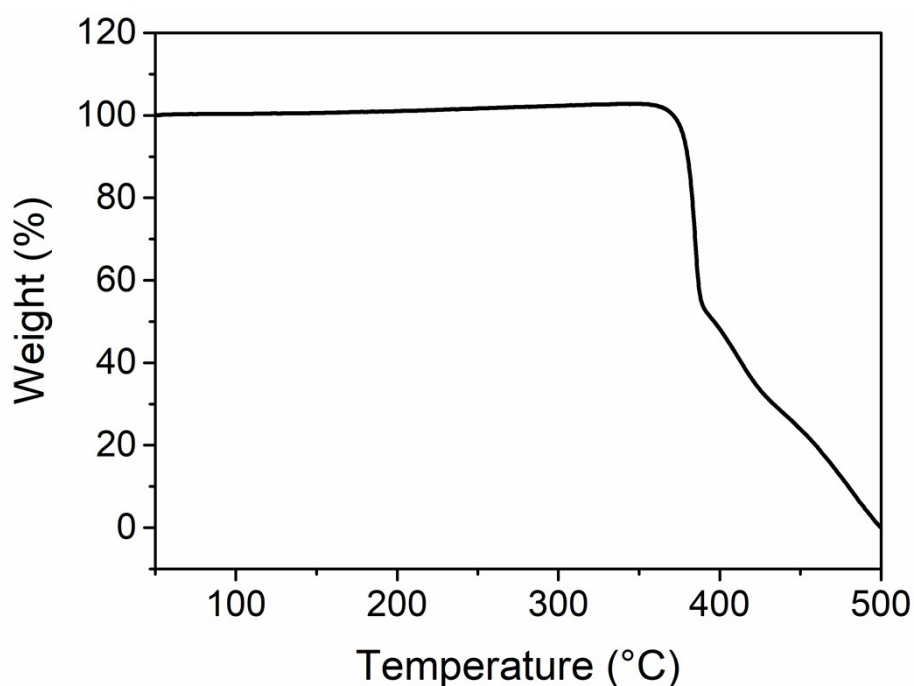


**Figure S1.** TGA curve for FPIC6.

#### 4. Temperature-dependent UV-vis spectra

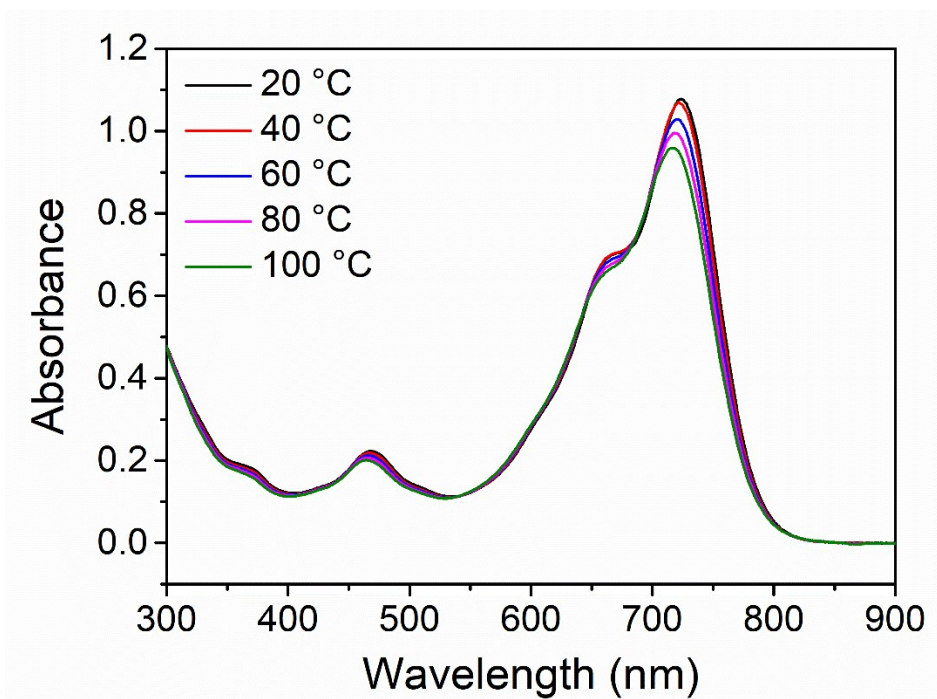


**Figure S2.** Temperature-dependent UV-vis spectra of FPIC6 in chlorobenzene solution ranging from 20 °C to 100 °C.

#### 5. CV

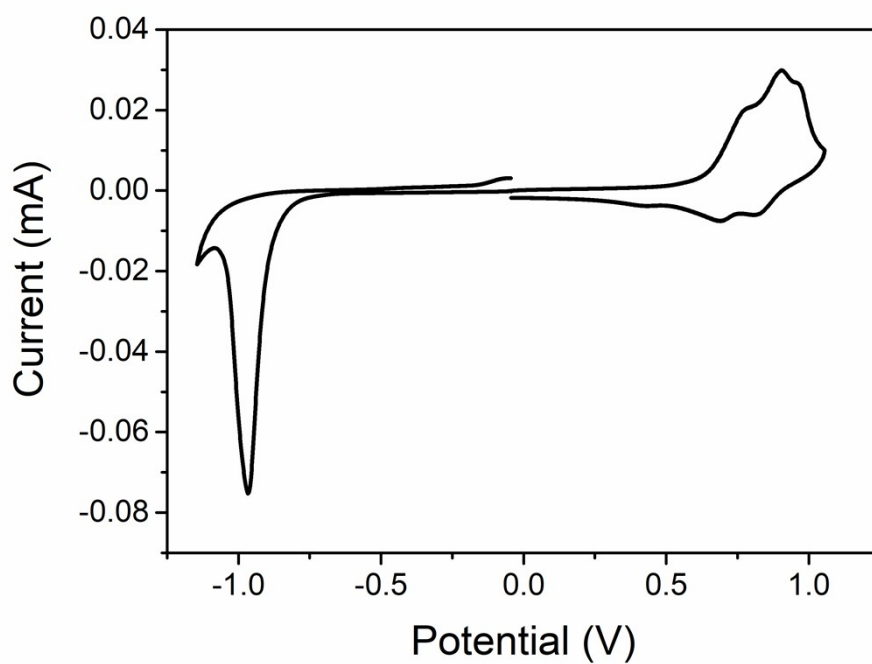


**Figure S3.** Cyclic voltammogram for FPIC6.

## 6. Density functional theory calculations

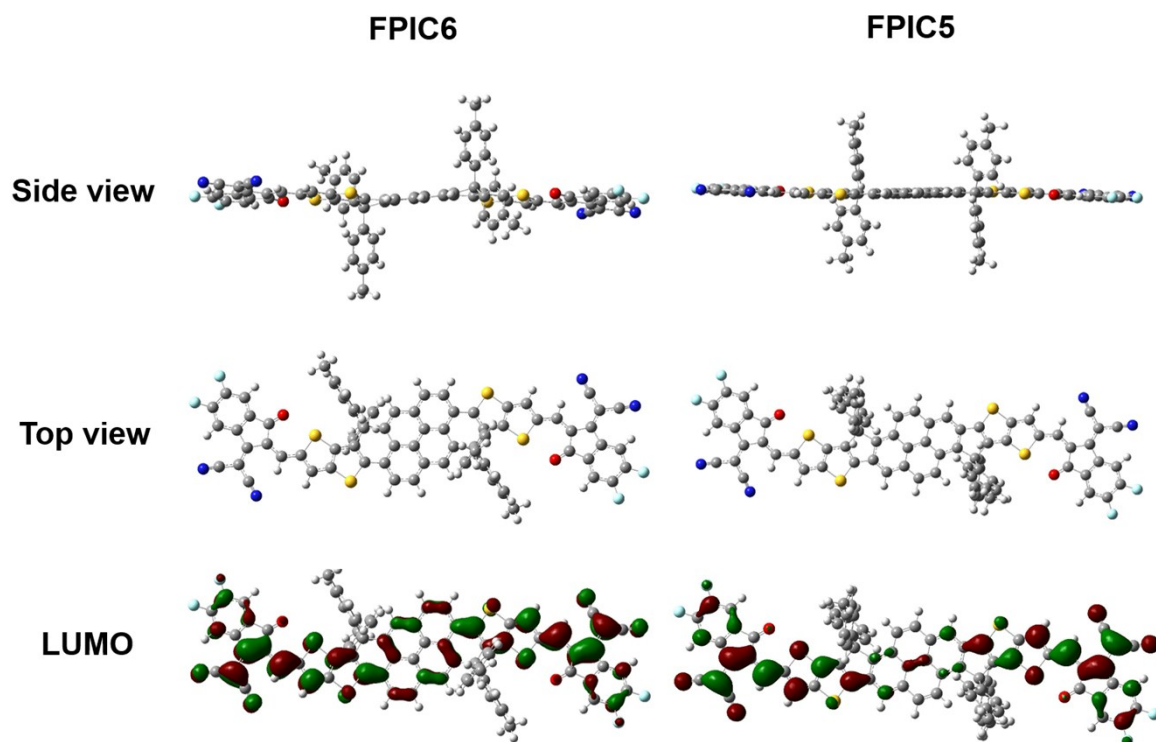


Figure S4. Optimized molecular conformations and LUMO for FPIC6 and FPIC5.

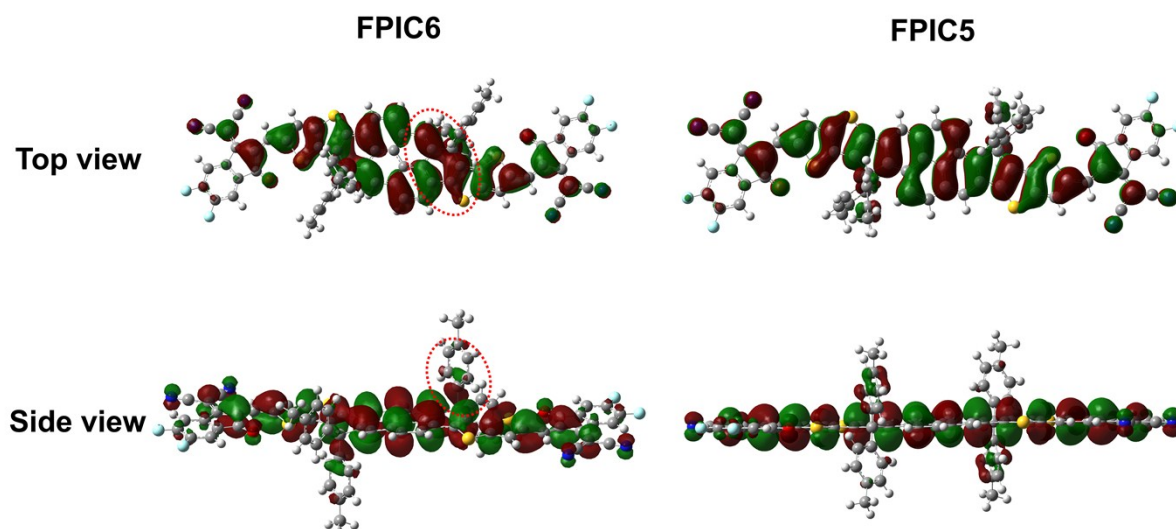


Figure S5. Optimized HOMO for FPIC6 and FPIC5.

## 7. Optimization of device performance

**Table S1** Optimization of D/A ratio for PTB7-Th:PFIC6 inverted solar cells.<sup>a</sup>

D/A	$V_{oc}$	$J_{sc}$	FF	PCE
[w/w]	[V]	[mA/cm <sup>2</sup> ]		[%]
1:1.0	0.79	20.22	0.59	9.43
1:1.5	0.79	20.61	0.61	9.91
1:2.0	0.79	20.10	0.55	8.81

<sup>a</sup> Blend solution: 9 mg/mL in CHCl<sub>3</sub>; spin coating: 4000 rpm.

**Table S2** Optimization of additive for PTB7-Th:PFIC6 inverted solar cells.<sup>a</sup>

additive	$V_{oc}$	$J_{sc}$	FF	PCE
[w/w]	[V]	[mA/cm <sup>2</sup> ]		[%]
Without	0.79	20.61	0.61	9.91
1% DPE	0.78	20.57	0.63	10.12
1% CN	0.77	21.99	0.66	11.18
1% DIO	0.78	20.34	0.66	10.39

<sup>a</sup> Blend solution: D/A= 1:1.5, 9 mg/mL in CHCl<sub>3</sub>.

## 8. Absorption spectra of PTB7-Th:PFIC6 blend films

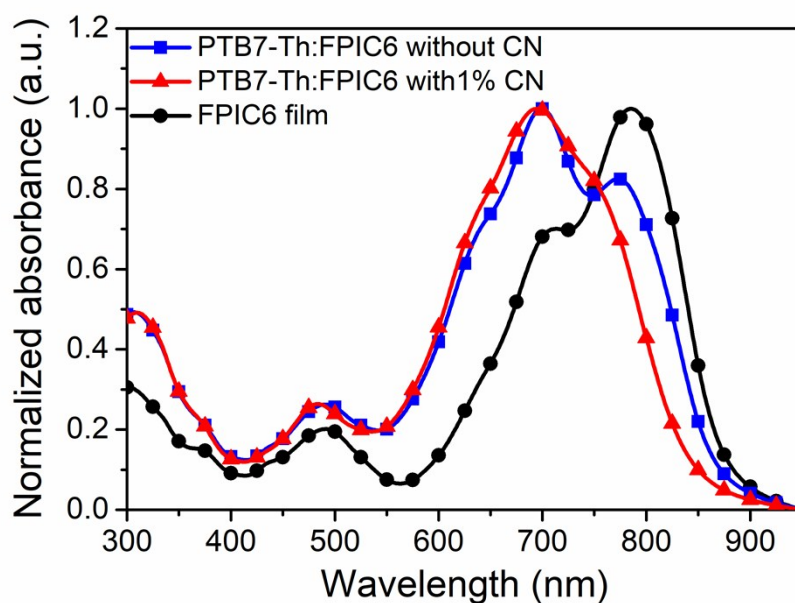


**Figure S6.** Absorption spectra of PTB7-Th:FPIC6 blend films without or with 1% CN, and pure FPIC6 film.

## 9. XRD

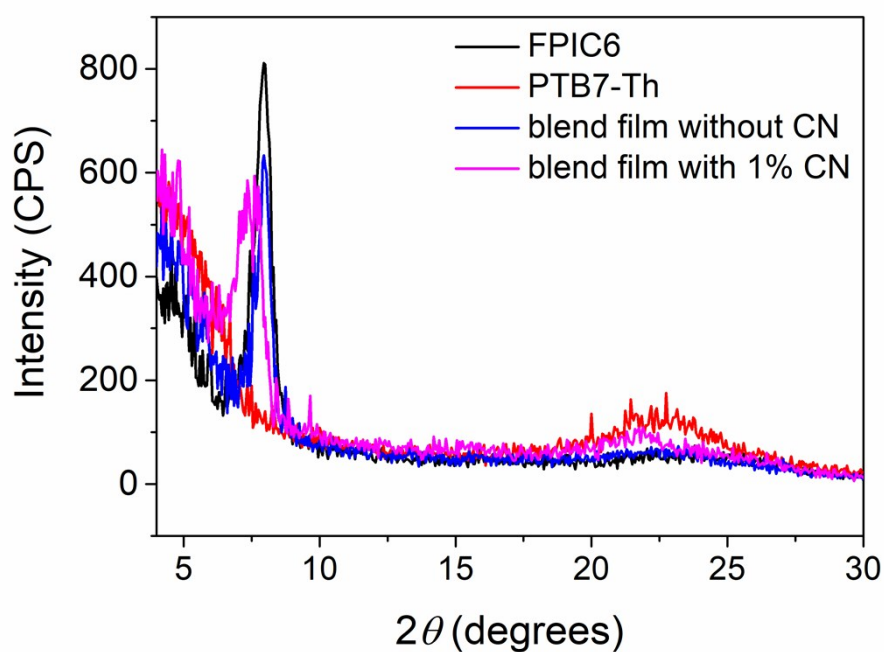


**Figure S7.** XRD patterns for FPIC6, PTB7-Th, and PTB7-Th:PFIC6 blend films without or with 1% CN.

## 10. DSC

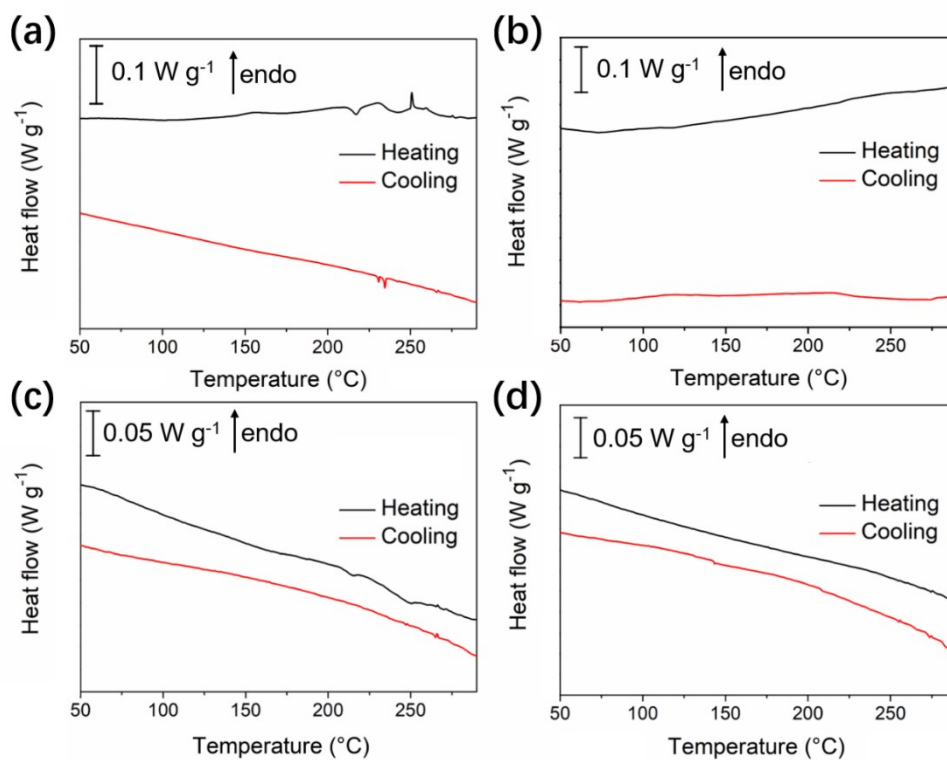


**Figure S8.** DSC curves of (a) FPIC6, (b) PTB7-Th, (c) PTB7-Th:FPIC6 without CN, and (d) with 1% CN.

## 11. PL spectra

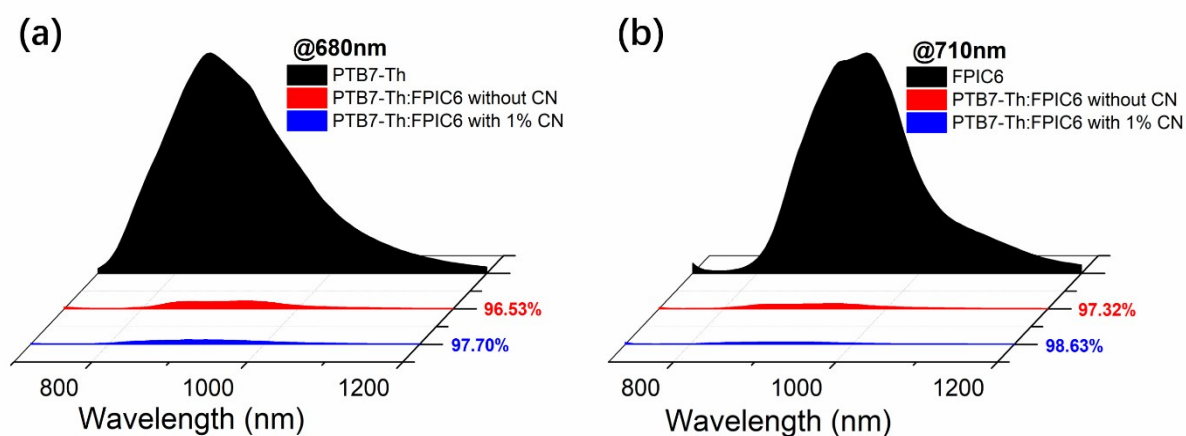


**Figure S9.** PL spectra of PTB7-Th and FPIC6 pure films, as well as PTB7-Th:FPIC6 blend films without or with 1% CN excited at (a) 680 nm, and (b) 710 nm.

## 12. Space charge limited current (SCLC) measurements

Charge carrier mobility was measured by SCLC method. The mobility was determined by fitting the dark current to the model of a single carrier SCLC, which is described by:

$$J = \frac{9}{8} \epsilon_0 \epsilon_r \mu \frac{V^2}{d^3}$$

where  $J$  is the current density,  $\mu$  is the zero-field mobility of holes ( $\mu_h$ ) or electrons ( $\mu_e$ ),  $\epsilon_0$  is the permittivity of the vacuum,  $\epsilon_r$  is the relative permittivity of the material,  $d$  is the thickness of the blend film, and  $V$  is the effective voltage,  $V = V_{\text{appl}} - V_{\text{bi}}$ , where  $V_{\text{appl}}$  is the applied voltage, and  $V_{\text{bi}}$  is the built-in potential determined by electrode work function difference. Figure S10 shows  $J^{0.5}$ - $V$  curves for the hole-only devices and the electrons-only devices, respectively.

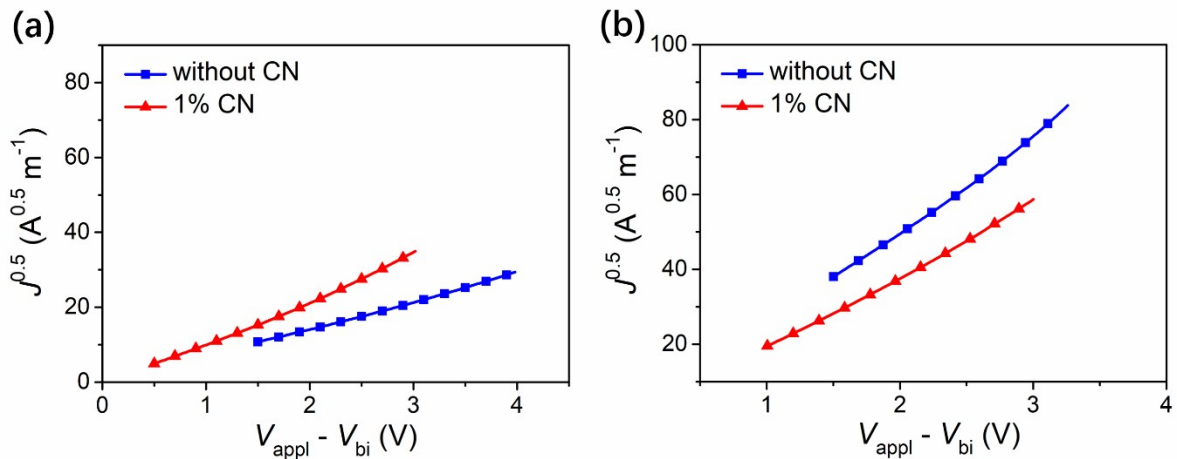


**Figure S10.**  $J^{0.5}$ - $V$  curve plots for (a) electron-only and (b) hole-only devices based on PTB7-Th:PFIC6 blend films without or with 1% CN (in the dark).

**Table S3** Mobilities for PTB7-Th:PFIC6 blend films.

Blend films	$\mu_e$	$\mu_h$	$\mu_h/\mu_e$
	$[\text{cm}^2 \text{V}^{-1} \text{s}^{-1}]$	$[\text{cm}^2 \text{V}^{-1} \text{s}^{-1}]$	
Without CN	$2.7 \times 10^{-5}$	$5.24 \times 10^{-4}$	19.4
With 1% CN	$6.2 \times 10^{-5}$	$2.80 \times 10^{-4}$	4.51

### 13. AFM height images

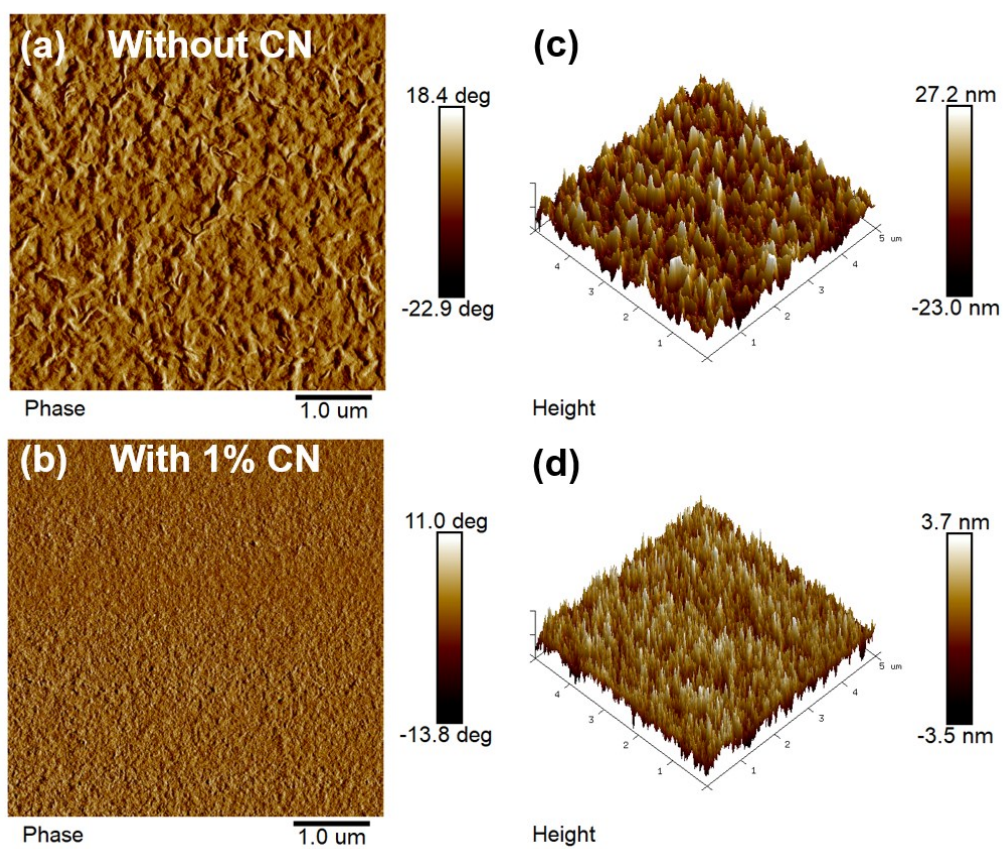


**Figure S11.** AFM (a, b) phase images and (c, d) height images of PTB7-Th:FPIC6 blend films without CN (above) or with 1% CN (bottom).

### References

- [1] Y. Sun, J. H. Seo, C. J. Takacs, J. Seifert and A. J. Heeger, *Adv. Mater.*, 2011, **23**, 1679.